FRACTURE RESISTANCE AND FAILURE CHARACTERISTICS OF AISI 304 / SA508 BIMETALLIC WELD IN DUCTILE REGIME

P. Nevasmaa, A. Laukkanen and U. Ehrnstén

VTT Manufacturing Technology
P.O. Box 1704, FIN-02044 VTT

ABSTRACT

Bimetallic welds impose a challenge to fracture mechanics in the comprehension of factors for the failure and to the reliable performance of materials characterisation. Welds can be manufactured using several metallurgical design concepts and the quantitative fracture mechanical properties related to different procedures remain imponderable. At present the knowledge of homogeneous weldments is utilised for design, and no detailed methods exist for appraising approvable assessment to structural integrity.

The paper presents results of fracture mechanical characterisation and fracture micromechanisms analysis for AISI 304-SA508 bimetallic weld with Nickel-enriched buttering. The experiments are complemented with numerical simulations for near crack tip conditions to perceive the failure behaviour. The materials characterisation consisted of tensile testing and fracture resistance (J-R) curve determination using small specimen test techniques. The results present the degree of linear and non-linear mismatch across the weldment and the associated fracture toughness. The weld fusion boundary area was found to dominate the fracture process due to local brittle zones and severe mismatch, especially for cracks placed to the ferritic steel HAZ close to the steel-buttering interface. The asymmetricity of plastic deformation, local crack tip constraint conditions and state of mixed-mode loading are concluded to control the crack initiation and propagation behaviour. Depending on crack placement relative to microstructure, material mismatch induced-constraint and state of mixed-mode loading were seen to dominate over geometry entailed changes in stress state. Micromechanisms of fracture were found to correlate with the numerical predictions made on the basis of local material properties.

INTRODUCTION

Differences in mechanical properties of the various microstructural regions of bimetallic weld, as well as in physical properties of the two dissimilar materials can promote in-service failure of welded structures. For ensuring safe operation, reliable material's property data are required to be applied in structural integrity assessment [1,3].

With respect to materials characterisation, not only there exist two mechanically (and physically) different materials, but also, due to the heat-affected zone (HAZ), fusion boundary (weld interface) and the buttering, a gradient in material properties in terms of microstructural constituents and local chemical compositions. The analysis work therefore requires extensive characterisation of material properties across the weld interface [1,2,4].

Buttering of the ferritic steel with a 2-3 mm thick layer of suitable intermediate material prior to final welding is a common procedure employed for bimetallic welds in power plant applications. Overalloying with Ni, e.g. 309L grade filler metal is used to reduce the toughness degradation resulting from carbide precipitation currently faced with matching austenitic filler metals [3].

MATERIALS AND EXPERIMENTS

The base materials comprise ferritic low-alloy steel SA508 and austenitic stainless steel AISI 304. As filler metals, over-alloyed Ni-enriched E 309L (24 % Cr-12 % Ni) was used for the 1st buttering layer, whilst matching E 308L (18 % Cr-8 % Ni) was used to deposit the buttering layers and to complete the final weld. The weld configuration is presented in Fig. 1.

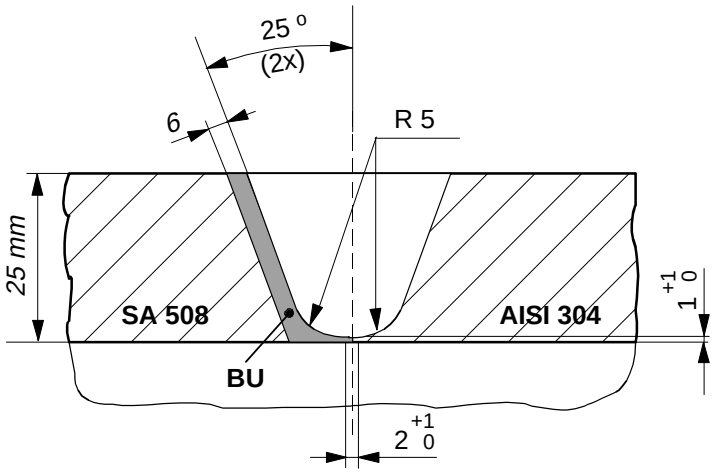

Figure 1: Bimetallic weld configuration.

Material's tensile properties and fracture initiation and crack growth data are typical inputs in structural integrity analysis. Mechanical testing consisted of *tensile tests, fracture toughness tests* and *metallographic examination* including *fractography*. The need to precisely locate the crack tip favoured the use of sub-sized specimens.

Tensile Testing

The use of *miniature flat-bar specimens* (1.0∗2.0mm) aimed at producing data on yield strength, ultimate tensile strength, elongation etc. from the different weldment regions. The purpose of using *miniature round-bar specimens* (∅ = 2.0-5.0 mm, L = 5 ∗ ∅) was to measure the true stress-strain curves, as well as to provide data on plastic deformation beyond yielding. All tests were carried out at room temperature.

Fracture Toughness Testing

For deriving the fracture resistance (J_R) curves, testing was carried out according to the ASTM E1737-96, using partial unloading compliance technique with side-grooved, sub-sized specimens (10∗10∗55 mm^3). The *weld metal*, *1st buttering layer*, *fusion boundary/CGHAZ* and the *outer HAZ* of the ferritic steel were examined. The specimens were pre-fatigued prior to testing. All tests were carried out at room temperature, except in the cases where the occurrence of unstable crack growth prevented any further ductile crack growth. When this occurred, testing temperature was lifted in order to meet ductile crack growth conditions.

Metallographic Examination and Fractography

The weld microstructures were investigated using optical microscopy and scanning electron microscopy (SEM). Metallography was performed to reveal the formation of inhomogeneous microstructural regions, if these existed. Fracture surfaces of the fracture toughness test specimens were examined using SEM, with the aim at explaining the micro-mechanisms of fracture and the microstructural path of the crack growth. The cross-sections of the fracture surfaces were occasionally investigated in order to correlate the observed crack path to the microstructure.

EXPERIMENTAL RESULTS

Mechanical Property Data

The fracture toughness test data according to ASTM E1737-96 in terms of fracture initiation values (J_{IC}, K_{JC}), crack growth parameters for a power-law fit (C, m) and the fracture/crack growth mode are presented in Table 1. Results of the tensile tests using miniature flat-bar specimens are presented in Table 2.

TABLE 1
FRACTURE TOUGHNESS TEST DATA USING SUB-SIZED SPECIMENS.

Specimen No	Testing Temperature [°C]	Notch location	Notch orientation	J_{IC} (*J_c) [kN/m]	K_{JC} [MPa√m]	C	m	Fracture/ Crack growth mode
BIM11	150	HAZ	T	207	213	296	0.46	ductile
BIM12	150	HAZ	L	402	297	455	0.35	ductile
BIM21	150	FL	T	125	166	186	0.38	ductile
BIM22	25	FL	L	337(*	272	-	-	**unstable**
BIM31	25	BL	T	229	224	316	0.45	ductile
BIM32	25	BL	L	158	186	262	0.55	ductile
BIM41	150	HAZ	L	263	240	350	0.45	ductile
BIM42	150	HAZ	T	250	234	317	0.35	ductile
BIM51	150	FL	L	363(*	282	-	-	**unstable**
BIM52	100	FL	T	153(*	183	-	-	**unstable**
BIM61	25	BL	L	165	190	268	0.54	ductile
BIM62	25	BL	T	544	346	†	†	ductile
BIM71	25	WM	L	295	255	398	0.53	ductile
BIM72	25	WM	T	195	207	323	0.62	ductile
BIM81	25	WM	T	161	188	326	0.77	ductile
BIM82	25	WM	L	242	231	353	0.55	ductile

(* : J_c and K_{Jc} are given instead of J_{IC} (K_{IC}) because of failure in an unstable manner
HAZ: ferritic steel heat-affected zone (FL + 2…3 mm)
CGHAZ: coarse-grained heat-affected zone of the ferritic steel
FL: fusion boundary / coarse-grained HAZ (FL + ≤ 0.5 mm)
BU: buttering layer (FL - 1…2 mm)
WM: weld metal (centreline)
T: notch and crack growth in section/weld thickness direction (from outer to inner surface)
L: notch and crack growth parallel to the weld in longitudinal (welding) direction
†: high initiation toughness prevented power-law fitting

TABLE 2
TENSILE TEST RESULTS USING FLAT-BAR MINIATURE SPECIMENS.

Test Serie N:o	Specimen orientation	Specimen Location	Tested weld region	$R_{p0.2}$ [MPa]	R_M [MPa]	A_5 [%]	A_{tot} [%]
Serie 1	L	upper part root region	WM, cap WM, root	347 - 388 452 - 507	513 - 541 580 - 659	34 - 52 32 - 42	43 - 58 39 - 48
Serie 2	T	upper part root region	WM, cap WM, root	363 - 390 405 - 434	531 - 560 590 - 604	31 - 37 21 - 28	39 - 43 28 - 40
Serie 3	L	mid-thickness region	WM BU CGHAZ HAZ	378 - 407 364 - 364 683 490 - 522	532 - 566 530 - 579 792 642 - 661	33 - 45 40 - 42 8 7 - 9	41 - 55 48 - 49 16 14 - 17
Serie 4	L	mid-thickness / root region	WM BU CGHAZ HAZ	425 370 - 413 725 515 - 515	555 551 - 608 827 659 - 660	39 31 - 39 8 8 - 8	45 37 - 46 14 14 - 17
Serie 5	T	mid-thickness / root region	WM - BU BU - HAZ	349 - 392 365 - 386	514 - 545 534 - 562	23 - 38 12 - 16	35 - 52 22 - 28

L : specimen parallel to the weld in the longitudinal (welding) direction
T : specimen transverse to the weld (and welding direction)

Metallographic Analyses
Martensite was observed as non-continuous islands (MNZ) along the fusion boundary at the weld interface. The width of the MNZ layer was 0.02-0.05mm. Immediately next, a 0.02-0.05mm wide decarburised zone (CDZ) was observed in the ferritic steel CGHAZ. In a ≈0.04mm wide zone in the immediate vicinity of the fusion boundary, the 1st buttering layer revealed a grain-type microstructure with visible grain boundaries, whereas the rest of the weld metal/buttering comprised a dendritic microstructure. No δ-ferrite was observed in this narrow layer with a grain structure, thus resembling the FAZ.

Fractographic Studies
Of the 4 fracture toughness specimens with the crack tip locating at the fusion boundary area, three (BIM22, BIM52, BIM51) showed unstable crack growth, whilst one (BIM21) exhibited ductile crack growth.

The fractography of BIM22, BIM 52 and BIM51 revealed that cracking had initiated in a ductile manner by *dimple coalescence* mechanism. Further propagation has occurred by *quasi-cleavage*, *interdendritic/grain boundary* and, finally, by *ductile fracture* mechanisms. A distinct feature was that the crack growth did not follow the plane of the pre-fatigue crack, but formed a quite steep step towards the weld interface soon after the initiation. The fractography of BIM21 without any crack growth instability revealed mainly *ductile fracture*. The plane of crack growth was much closer to the plane of the original pre-fatigue crack than in the case of the other 3 specimens above.

The distances of the pre-fatigue crack tip from the fusion boundary differed between the 4 specimens, being 0.7mm (BIM22), 0.4mm (BIM52), 1.2mm (BIM51) and 0.1mm (BIM21). The distances were measured from the cross-sections and correspond to the findings of the fractographic investigations. Thus, the pre-fatigue crack tip in BIM21 showing ductile crack growth located in almost at the weld interface, whereas the crack tip in BIM22, BIM52 and BIM51 which exhibited crack growth instability located further off in the coarse-grained/small-grained HAZ.

DISCUSSION

Strength Properties of Bimetallic Weld
The tensile test results demonstrate that the miniature flat-bar specimens taken from various weld depths and in two orientations are suitable for the characterisation of the strength and ductility of the different microstructural regions of bimetallic weld. For determining true stress-strain curves for these regions, a round-bar specimen geometry appears appropriate. In combination with suitable monitoring techniques, round-bar specimens can be used to characterise local plastic deformation behaviour more adequately, such as diametral contraction and necking radius.

Strength behaviour according to miniature flat-bar specimens taken in the transverse direction and hence containing various microstructures, is determined by the strength of the weakest region. The results show that the surrounding harder regions were unable to strengthen the weaker region. This is attributed to the small width/thickness (w/t) ratio of 1.5-2.0 applied. Specimens with higher w/t ratios of 5-8 are likely to express the restraining effect of the surrounding higher strength microstructures.

Whilst the strength properties of the weld metal and the buttering are likely to be very similar, the strength of the CGHAZ of nearly 2 times of that of the weld/buttering was recognised. The elongation in the CGHAZ, in turn, remained only 1/4-1/5 of that of the weld metal and the buttering. Consequently, a substantial mismatch in strength and ductility results in bimetallic welds, which is quantified on the basis of different types of tensile tests. The results in Fig. 2 illustrate the undermatching of the joint across the fusion line (solid curves). The strain hardening exponents fitted from the true stress-strain curves present the decrease of deformation capability of the HAZ when compared to the SA508 base material. The austenitic weld metal, and especially the austenitic base material, is in a league of their own with respect to strain hardening behaviour.

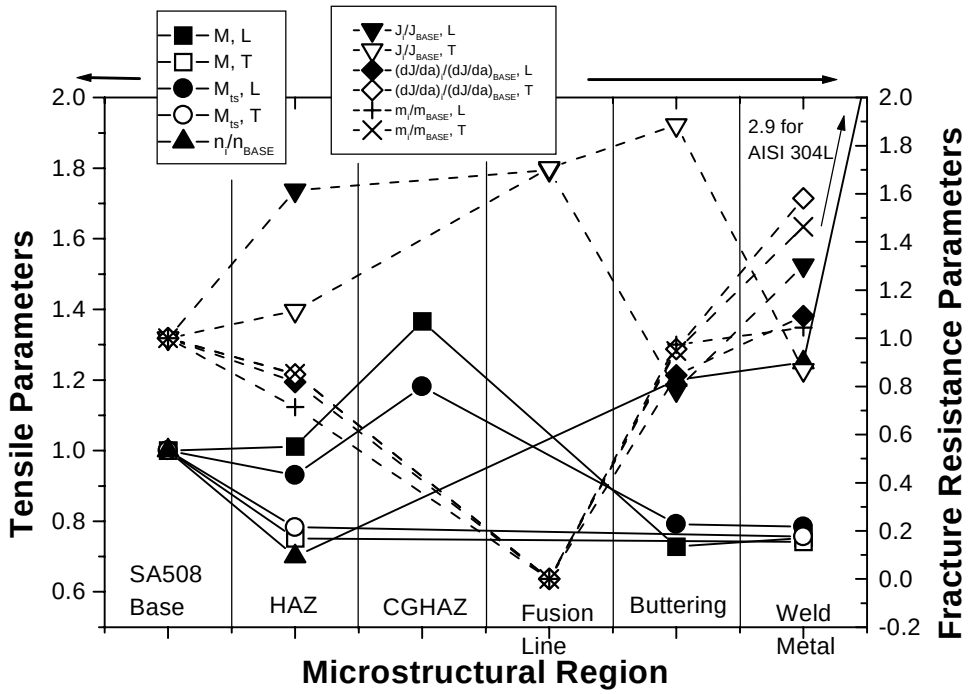

$M = \sigma_{ys}^{i} / \sigma_{ys}^{BASE}$, $M_{ts} = \sigma_{ts}^{i} / \sigma_{ts}^{BASE}$, $n \Leftrightarrow$ strain hardening exponent, $\sigma_{ys} \Leftrightarrow$ yield strength and $\sigma_{ts} \Leftrightarrow$ tensile strength.

Figure 2: Comparison of tensile and fracture toughness test results in different regions of bimetallic weld.

Fracture Toughness of Bimetallic Weld

For the majority of the weldment regions fully ductile crack growth was encountered. This demonstrated sufficient fracture resistance of the microstructures in these regions. The fracture resistance results for initiation and propagation are summarised in Fig. 2 along with the results for variations of tensile properties. The increase of mismatch associated to the near regions of the fusion line and the differences in deformation behaviour characterised by the strain hardening exponent are found to effect the fracture resistance drastically (as in [5]). The plasticity during crack propagation, characterised by m and dJ/da, decreases to its extreme of zero near the fusion line, which is found to experience the highest values of both linear and nonlinear mismatch. The fact that the occurrence of practically brittle fracture is associated with relatively high values of initiation fracture toughness is quite likely related to crack placement and to deviation effect. The crack deflection causes the specimen to store additional driving force for crack propagation, which manifests it as unstable brittle-type fracture after ductile initiation, as soon as weaker microstructures are found from the crack path. This occurs when the crack is closer to the weld interface. Unstable crack growth without any ductile tearing was repeatedly recognised in the case of the fusion boundary area/ferritic steel HAZ.

Characteristics and Micromechanisms of the Observed Fracture Modes

Unstable crack growth preceded by ductile initiation

In this failure mechanism a propagating fracture, once initiated in a ductile manner in the CGHAZ (where the crack tip was located), deviated in a relatively sharp angle towards the weld interface which was several millimetres aside from the original crack tip. This demonstrates the high driving force for crack propagation and final failure, as well as the criticality of this 'weak' fracture path in the studied bimetallic weldment.

The high initiation toughness, but otherwise unstable failure is attributed to the fact that while the crack tip is located at an adjacent microstructure and the portion of brittle phase is in macroscopic terms low, the initiation can be interpreted directly as work performed at the 'near crack tip' regions (in softer microstructures) <u>without</u> effectively growing the crack. Then, at a certain stage the crack can propagate either through the asymmetrically developed plastic zone or via damage formation directly to the local brittle microstructure (LBZ) transferred by the deforming microstructures (crack deviation).

The significance of mismatch can be related to the *failure behaviour of 'brittle' constituents as an increase in constraint* (if linear mismatch is concerned), or the *deformation experienced by the softer regions and the resulting compatibility requirements set to the harder microstructures* (in the case of elastic-plastic mismatch). For the crack locating in the CGHAZ, the plastic deformation of the interface associated to the CDZ and the FAZ can cause a large increase in local plasticity in regions surrounding the LBZs. This manifests itself as degradation in toughness. In the case of linear-elastic mismatch and crack located near the fusion boundary, the situation is, in turn, directed towards a typical weakest link controlled 'brittle' or 'unstable' failure promoted by a constraint increase, which is thereby dependent on the division and relative proportions of different microstructures at the near-crack-tip volumes.

Consequently, *unstable crack growth* initiated from the CGHAZ in a ductile manner can be viewed as a mixed-mode failure, where the asymmetricity originates primarily from the elastic-plastic mismatch of different constituents. The distributions of plastic strain will follow the associated mismatch gradient and straining is promoted at softer regions, while the stress state will remain generally at a high level due to mismatch and the presence of elastic microstructures (i.e. harder regions). After the deviation of the crack tip from the CGHAZ to the fusion boundary area (interface), the situation remains practically the same in terms of load state and plasticity, since the state of mismatch is not significantly altered. Thus, the crack propagation will occur in an unstable fashion as long as suitable combination of local brittle hard regions (MNZ), together with surrounding softer zones (CDZ, FAZ) remains, and the weakest linear-elastic structures will drive the failure process.

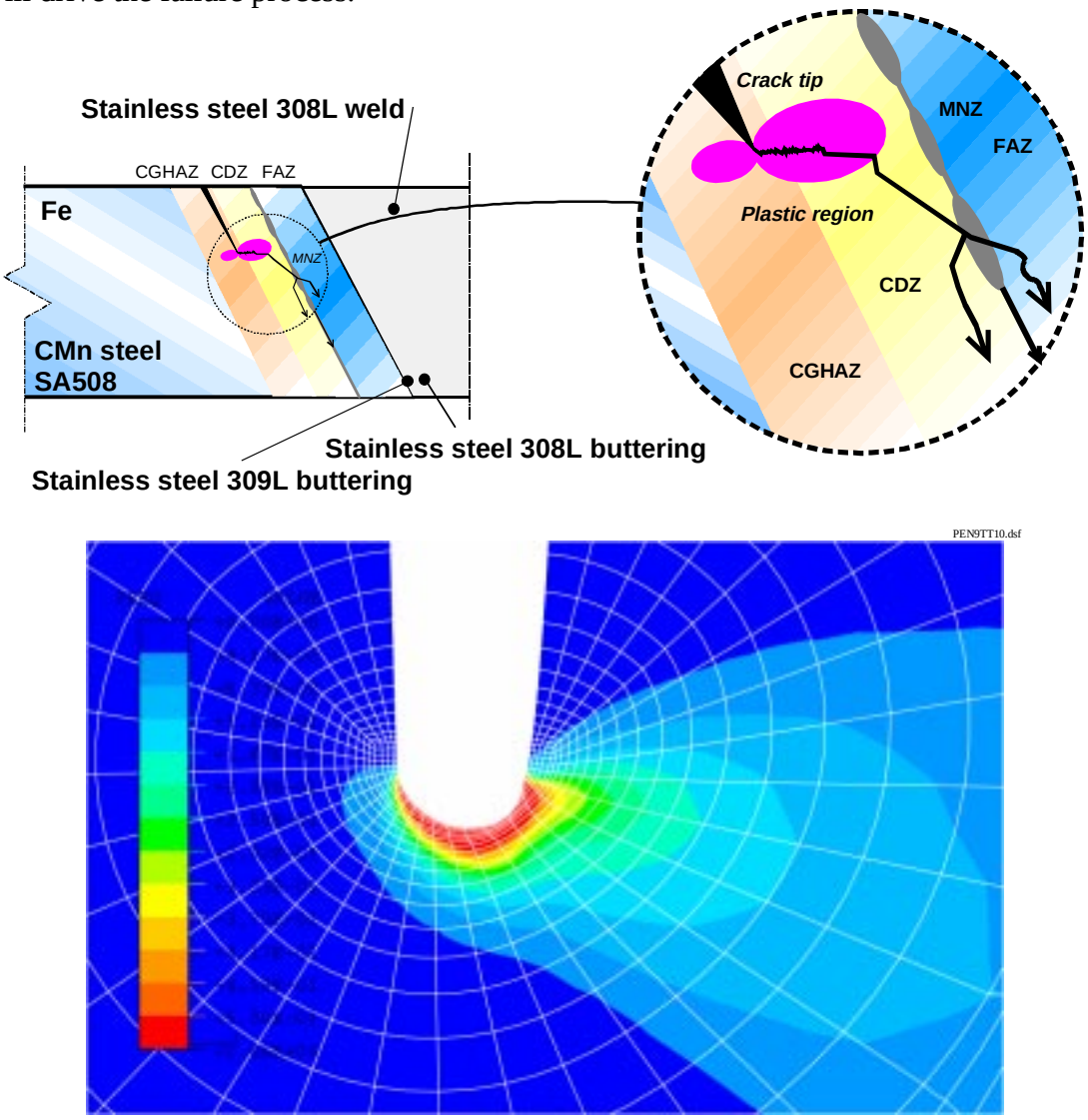

Figure 3: Schematic illustration and finite element results for equivalent plastic strain of the micro-mechanism associated with unstable crack growth.

The occurrence of '*unstable crack growth without ductile tearing*' in Fig. 3 can be explained according to the following micro-mechanical model: (i) original notch tip in the CGHAZ, (ii) development (under external load) of an *asymmetric plastic region* at the notch tip towards the adjacent CDZ of lower strength,

as a result of strength mismatch between the CGHAZ and the CDZ, (iii) ductile initiation of a crack in the CGHAZ, (iv) crack deviation through the softened CDZ by quasi-cleavage to the weld interface containing discontinuous MNZ, (v) cleavage fracture of the MNZ (or de-bonding of the interface between the matrix and the MNZ) representing a 'local brittle zone' and (vi) further crack propagation either along the interface, by deflecting to the FAZ (interdendritic fracture), or by deflecting to the CDZ (quasi-cleavage). Fig. 3 also presents corresponding an equivalent plastic strain distribution as given by finite element analyses (details given in ref. [6]), which highlights the development of near crack tip region deformation states under mismatching conditions.

Low toughness ductile fracture

The occurrence of '*low toughness ductile fracture*' at the fusion boundary, see Fig. 4 for schematic model and finite element results, was associated with the original notch locating closer to the interface than was the case with unstable crack growth. The reason why at least nominally ductile failure occurs, in contrast to totally unstable fracture event, can be inferred from the level of driving force at crack initiation and local material properties. If the crack tip is located in the CGHAZ, the (asymmetric) plasticity before final unstable fracture will give rise to a generally high level of driving force in terms of e.g. the J-integral, producing an energy supply leading to brittle/unstable failure after the crack deflection to the interface due to its inherent low ductility. If, however, the crack is located near or at the fusion boundary and hence closer to the interface, the failure can occur as ductile fracture with a generally low level of driving force. Thus, the difference is within the process zones between the two fracture events. Why ductile failure can occur in the latter case, can be explained by the fact that the MNZ is still to be interpreted as a local region consisting of brittle constituents, and the softened zones (CDZ, FAZ), although due to their microstructure are unable to entail significant plasticity, still behave as ductile materials.

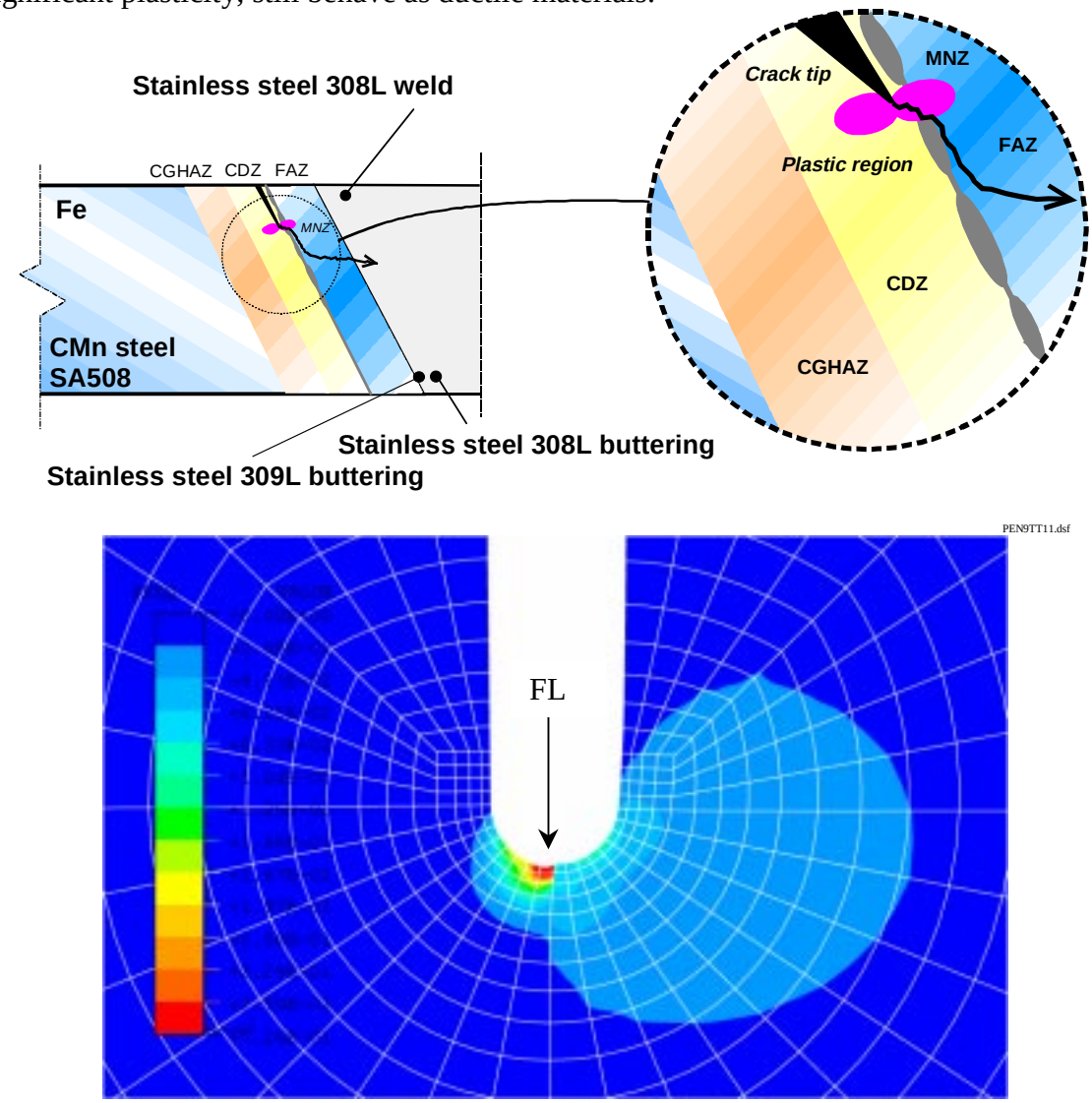

Figure 4: Schematic illustration and finite element results for equivalent plastic strain of the micro-mechanism associated with ductile crack growth.

The failure mode can be explained by the following micro-mechanical model, see Fig. 4: (i) original notch tip at the fusion boundary, (ii) development of a less asymmetric plastic region at the notch tip (under external loading, smaller volume of influence) than in the case of a notch tip locating in the CGHAZ, (iii) ductile initiation at the weld interface, (iv) crack deviation through the FAZ (in the 1st buttering layer) to the buttering/weld metal, and (v) ductile crack growth at the buttering/weld metal by ductile tearing.

SUMMARY AND CONCLUSIONS

Fracture toughness tests revealed fully ductile crack growth and adequate fracture resistance for the majority of weld regions. Unstable crack growth without ductile tearing was occasionally recognised in the case of the fusion boundary area. In these cases, the J_R -curves revealed substantial fracture resistance associated with the initiation stage, before the final failure took place in an unstable manner.

Fracture behaviour of each microstructure was satisfactorily characterised by using parameters J_{IC} (or K_{JC}) for describing fracture initiation, and *C*, *m* and *dJ/da* for describing subsequent fracture resistance and crack growth. Whilst *m* typically ranges from 0.4 to 0.6 irrespective of microstructure and temperature, the results suggest that *C* is not only material but also microstructure dependent. Tearing resistance *dJ/da* was found to correlate with *m* rather than either *C* or J_{IC}. In addition, *dJ/da* implied dependency on microstructure.

A combination of several adjacent microstructures: the *carbon depleted region* in the ferritic HAZ, the weld interface with discontinuous *martensitic regions* and the *fully austenitic region* in the 1st buttering layer, all with mismatching mechanical properties, was found responsible for unstable crack growth. Critical conditions were met when a crack located at the interface of two regions, of which one exhibited plastic behaviour while the other still behaved practically linear-elastically. Demonstrating these phenomena becomes possible when using small specimens that tend to favour a more accurate location of the notch in the desired microstructure. On the other hand, small specimen size may pose problems in terms of low constraint and limited measuring capacity. In the case of bimetallic welds, however, constraint due to microstructural mismatch/inhomogeneity is argued to play a more essential role in the fracture process than structure/geometry-induced constraint. Asymmetric load states (i.e. mixed-mode loading) can have a substantial effect in promoting local plastic strains. The results demonstrated that descriptive fracture toughness estimates can be obtained using sub-sized ($10*10*55$ mm^3) specimens.

REFERENCES

1 C. Faidy, G. Chas, S. Bhandari, C. Sainte-Catherine, R. Hurst, P. Nevasmaa, K. Schwalbe, W. Brocks, D. Lidbury and C. Wiesner: 'BIMET: Structural Integrity of Bi-Metallic Components'. Proc. of the "*FISA'97 Conference*", Luxembourg, 17-19 November 1997. Luxembourg: Nuclear Fission Safety (FISA) 1997. 7 p.

2 W.V. Vaidya, M. Kocak, M. Goldthorpe, C. Wiesner, P. Nevasmaa and R. Pelli: 'Evaluation of Fracture Toughness and Fatigue Crack Growth for Transition Welds at Non-Creep Temperatures - Task 1b Report'. GKSS Document No P3203F02#2 . GKSS Research Centre, Geesthacht, June 1998. 7 p + App 172 p.

3 D. Buckthorpe, C. Escaravage, P. Neri, P. Pierantozzi and D. Schmidt: 'Final Report CSC-WGCS/AG2 Study Contract on Bi-Metallic Weldments (ETNU-CT94-0133UK). Document No C9731/TR/002, Issue V02. NNC Ltd, April 1997.

4 W.V. Vaidya, M. Kocak, M. Goldthorpe, C. Wiesner, B. Houssin, S. Bhandari, P. Nevasmaa and A. Laukkanen: 'Evaluation of Fracture Toughness and Fatigue Crack Growth for Transition Welds at Non-Creep Temperatures - Tasks 1c & 1f Report'. GKSS Document No P3203F02#3. GKSS Research Centre, Geesthacht, September 1998. 6 p. + Apps 79 p.

5 A. Laukkanen: 'Effects of linear and nonlinear mismatch on assessment and failure behaviour of bimaterial joints'. VTT Manufacturing Technology, 1999, 96 p. + Apps.

6 A. Laukkanen and P. Nevasmaa: 'Local Approach Study on Fracture Mechanisms and Constraint Effects in a Bimetallic Weld'. VTT Manufacturing Technology, (to be published), 2000.